Supplementary Table 1

Tumor line	Tumor Type	p53 mutation	Other mutations
MDA-MB-468	Breast carcinoma	R273H	PTEN (gene del.) RB1 (null)
U373MG	Glioblastoma	R273H	CDKN2A (gene del.) CDKN2B (gene del.)
U251MG	Glioblastoma	R273H	CDKN2A (gene del.) CDKN2B (gene del.)
SF295	Astrocytoma	R248Q	PTEN (R233*) CDKN2A (gene del.) CDKN2B (gene del.) CCND1 (gene amp.)
HCC193	Non-Small Cell Lung Cancer	R248Q	CDKN2A (gene del.) RB1 (gene del.)
PC-9	Non-Small Cell Lung Cancer	R248Q	CDKN2A (missense mut.) EGFR (missense mut.) KRAS (missense mut.)
HCC1395	Breast carcinoma	R175H	PTEN (gene del.)
HCC1954	Breast carcinoma	Y163C	PI3KCA (H1047R)
BT-549	Breast carcinoma	R249S	PTEN (gene del.) RB1 (gene del.)
LN229	Glioblastoma	K164E	EGFR (gene amp.) CDKN2A (gene del.) CDKN2B (gene del.)
M059J	Glioblastoma	E286K	PTEN (frameshift) RB1 (gene del.l)
M059K	Glioblastoma	E286K	PTEN (frameshift) NF1 (Q1033R/F1037C) BRCA2 (gene del.)
U138MG	Glioblastoma	I232T/C242F	CDKN2A (gene del.)
SK-MEL-2	Melanoma	G245S	NRAS (Q61R) PIK3C3 (R768W) CCND1 (gen amp.)
SK-LMS-1	Sarcoma	G245S	NF1 (frameshift) CDKN2A (gene del.) CDKN2B (gene del.)
HCC1937	Breast carcinoma	R306*	PTEN (gene del.) BRCA1 (null)
HCC1806	Breast carcinoma	frameshift	
H1299	Non-Small Cell Lung Cancer	gene deletion	NRAS (Q61K)

Supplementary Table 1. Human tumor lines representing different tissue types and harboring the specific DNA contact (in blue), conformational (in red) missense or nonsense (in grey) p53 mutation indicated. Color coding followed throughout manuscript. The mutations indicated were obtained from TCGA databases [1].

Supplementary Table 2

ChIP qPCR			
Gene	**Relative to TSS**	**Forward**	**Reverse**
HMGCR	-2100	GAGGAAGCGGCACATGGA	TGGTATGGACACAAGGTAGAAAGG
	-1100	TTTTCAAGGTCGGGAGTAGATG	ACTTTTTCATATGCCACCTCCTTT
	-150	TGGGACTCGAACGGCTATTG	GAACAGGCACCGCACCAT
AchR		TCTGTCTCGGCAGCTGACAT	ACCACAAAAGATCAAGGTGAGTGA

qRT-PCR		
Gene	**Forward**	**Reverse**
GAPDH	CTCTGCTCCTCCTGTTCGAC	TTAAAAGCAGCCCTGGTGAC
CTGF	CCAATGACAACGCCTCCTG	TGGTGCAGCCAGAAAGCTC
CYR61	AGCCTCGCATCCTATACAACC	TTCTTTCACAAGGCGGCACTC
ANKRD1	CACTTCTAGCCCACCCTGTGA	CCACAGGTTCCGTAATGATTT
NF2	GCAGATCAGCTGAAGCAGGA	ACCAATGAGGTTGAAGCTTGGTA
LATS1	GTTAAGGGGAGAGCCAGGTCCT	TCAAGGAAGTCCCCAGGACTGT
LATS2	ACTTTTCCTGCCACGACTTATTC	GATGGCTGTTTTAACCCCTCA
HMGCR	GGCCCAGTTGTGCGTCTT	CGAGCCAGGCTTTCACTTCT
SQLE	CGTGCTCCTCTTGGTACCTCAT	CGGTCAAGGCGGAGATTATC
ROCK1	AGCAGAAGTGCAGAACCTCAAA	TACAGCTGTGTCCGATTCTGT
ROCK2	CCCATCAACGTGGAGAGCTT	TGCCTTGTGACGAACCAACT

Supplementary Table 2. Primer Sequences

Supplementary Figure 1

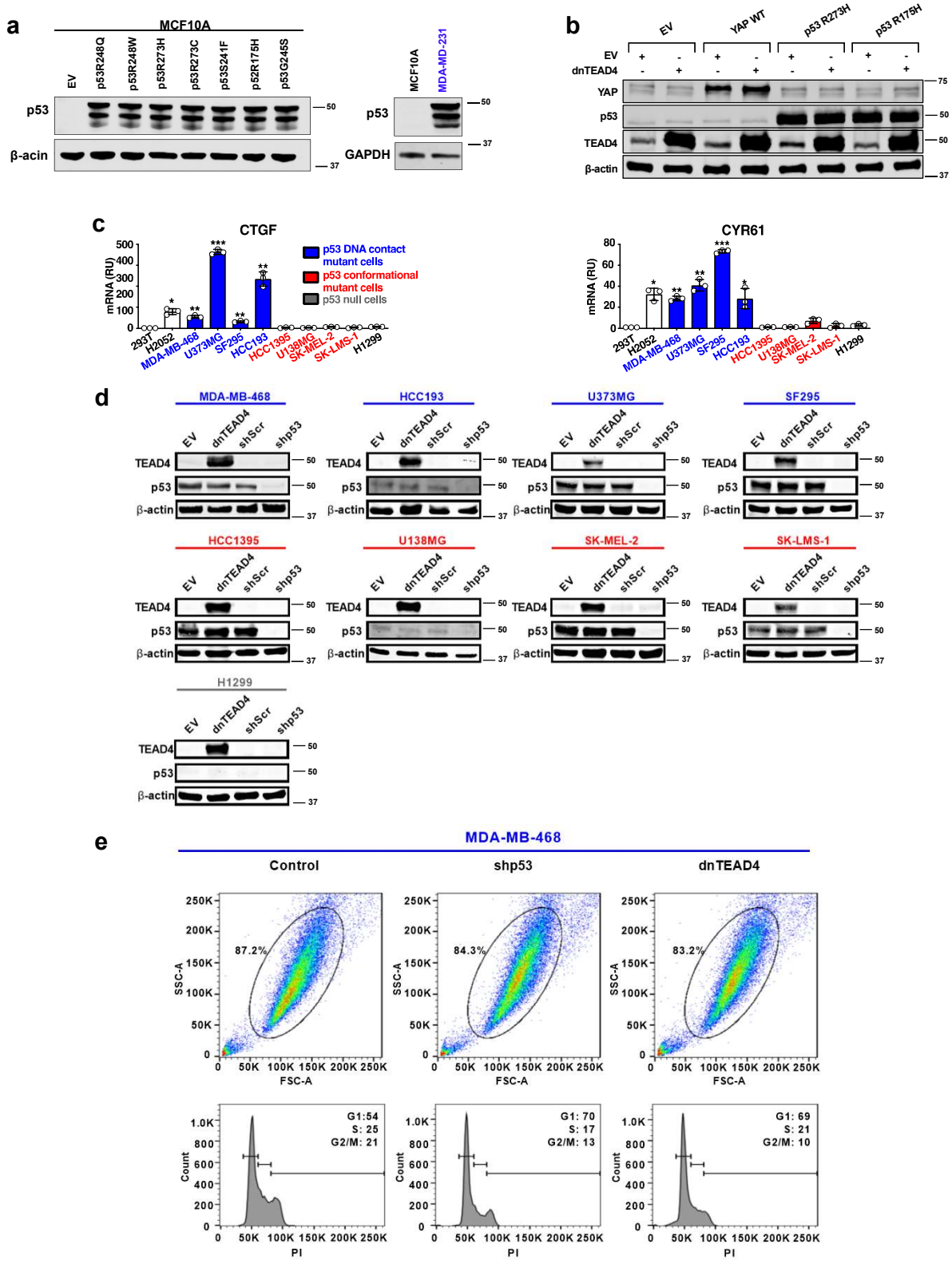

Supplementary Figure 1. p53 DNA contact mutants represent a class of TEAD/YAP upregulated tumors. (a) Western blot analysis of whole cell lysates from MCF10A cells stably expressing EV control or the indicated p53 mutants (left panel); or from MCF10A cells and MDA-MB-231 tumor cells (right panel). Lysates were probed with p53 antibody. **(b)** Western blot analysis of whole cell lysates from MCF10A cells stably expressing EV control, YAP WT or p53 R273H in the presence or in absence of dnTEAD4 stable expression. Lysates were probed with the indicated antibodies. β-actin was used as a loading control. **(c)** mRNA expression of TEAD/YAP target genes, CTGF and CYR61, by real time PCR in human tumor lines containing hot spot p53 DNA contact (in blue), conformational (in red), or null (in gray) mutations as specified in Supplemental Table 1. 293T (wt p53) and H2052 cells (wt p53 and NF2; LATS2 LOFs) served as negative and positive controls, respectively. **(d)** Western blot Western blot analysis of whole cell lysates from the indicated tumor lines containing p53 DNA contact (in blue) and conformational (in red) mutations and stably expressing EV control, dnTEAD4, shScr or shp53. Lysates were probed with the indicated antibody. β-actin was used as a loading control. **(e)** FSC-A/SSC-A profile with indicated gated cells and corresponding cell cycle profile by Propidium Iodide staining of MDA-MB-468 cells stably expressing EV control, shp53 or dnTEAD4. *p* values were derived using two tailed *t*-tests from means ± SD of $n=3$ independent experiments. $*p < 0.05$, $**p < 0.01$, $***p < 0.001$. Source data with actual calculated *p* values are provided as Source Data file.

Supplementary Figure 2

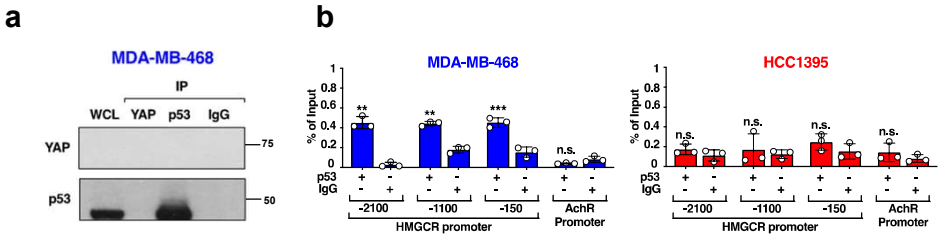

Supplementary Figure 2. **P53 and YAP do not interact in human tumor lines with p53 DNA contact or conformational mutations. (a)** Co-immunoprecipitation of endogenous p53 and YAP in MDA-MB-468 cells. IgG antibodies were used as a negative control. 10% of total cell lysate was used as Input. **(b)** ChIP analysis on HMGCR promoter in the indicated tumor lines. ChIP was performed with p53 or control immunoglobulin G (IgG) antibody and quantified by real-time PCR on the indicated promoter regions. Acetyl choline receptor (AchR) promoter was used as a negative control. *p* values were derived using two tailed *t*-tests from means ± SD of *n*=3 independent experiments. $^{**}p < 0.01$, $^{***}p < 0.001$. Source data with actual calculated *p* values are provided as Source Data file.

Supplementary Figure 3

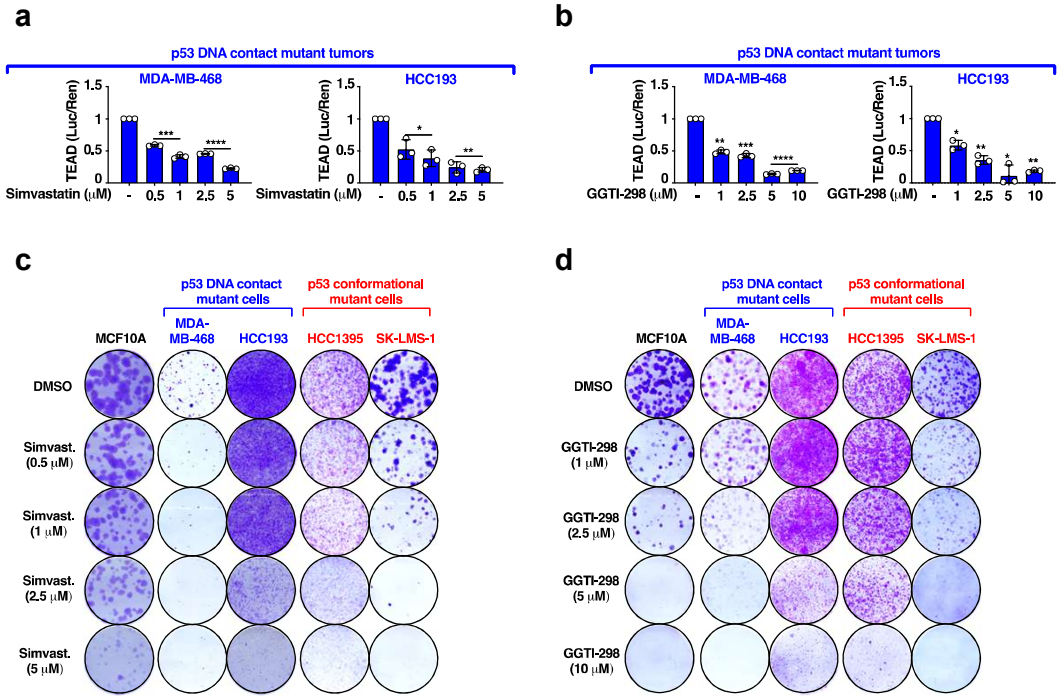

Supplementary Figure 3. Effects of Simvastatin and GGTI-298 on TEAD/YAP driven transcription and cell growth in human tumor lines harboring p53 DNA contact mutations. (a and b) TEAD reporter activity in the indicated tumor lines treated with DMSO or increasing concentrations of Simvastatin **(a)** or GGTI-298 **(b). (c and d)** Representative plates showing 2D colony formation by the indicated cell lines treated with DMSO or increasing concentrations of Simvastatin **(c)** or GGTI-298 **(d)** every 2 days for 14 days. *p* values were derived using two tailed *t*-tests from means± SD of *n*=3 independent experiments. **p* < 0.05, ***p* < 0.01, ****p* < 0.001, *****p* < 0.0001. Source data with actual calculated *p* values are provided as Source Data file.

Supplementary Figure 4

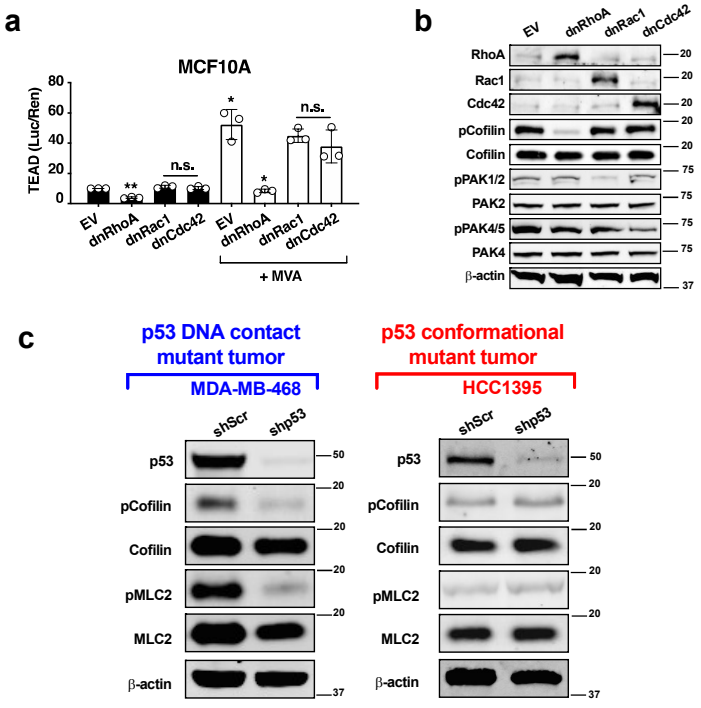

Supplementary Figure 4. RhoA activates TEAD/YAP transcription in MCF10A cells. (a) TEAD reporter activity in MCF10A cells transiently transfected with EV control, dnRhoA, dnRac1 or dnCdc42 in the presence or absence of 0.5 mM MVA for 24hrs. **(b)** Western blot analyses of whole cell lysates from MCF10A cells transiently transfected with EV control, dnRhoA, dnRac1 or dnCdc42 and probed with the indicated antibodies. β-actin was used as a loading control. **(c)** Western blot analyses of whole cell lysates from the indicated tumor lines and probed with the indicated antibodies. β-actin was used as a loading control. *p* values were derived using two tailed *t*-tests from means± SD of $n=3$ independent experiments. $*p < 0.05$, $**p < 0.01$. Source data with actual calculated *p* values are provided as Source Data file.

Supplementary Figure 5

a

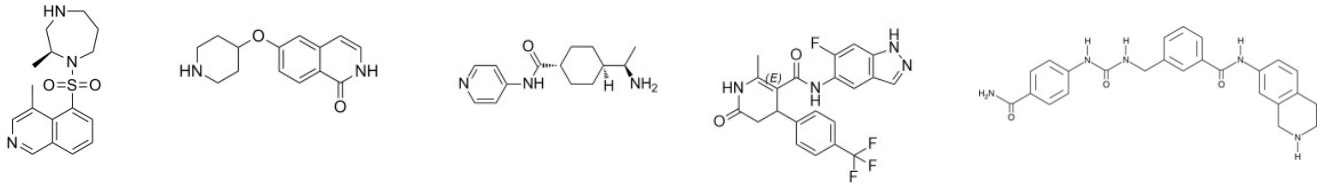

b

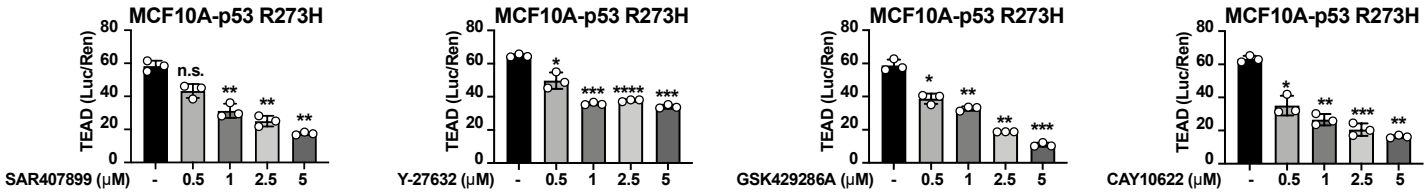

c

		ROCK1	ROCK2	PKA	PKC	PKG	CaMKII
H-1152	IC50 (μM)	0.006	0.016	0.63	9.27	3.26	10.1

		ROCK1	ROCK2	RSK	PKB	PKC
SAR407899	IC50 (μM)	0.102	0.135	>10	>10	5.4

		ROCK1	ROCK2	PKA	PKC	PKN
Y-27632	IC50 (μM)	0.22	0.14	25	73	3.1

		ROCK1	ROCK2	RSK	p70S6K
GSK429286A	IC50 (μM)	0.014	0.063	0.78	1.94

		ROCK1	ROCK2	44 other kinases
CAY10622	IC50 (μM)	0.006	0.004	>0.7

Supplementary Figure 5. ROCK inhibitors with different structures antagonize TEAD/YAP transcription activated by p53 DNA contact mutations in MCF10A cells. (a) Chemical structures of the ROCK inhibitors H-1152, SAR407899, Y-27632, GSK429286A and CAY10622. **(b)** TEAD reporter activity in MCF10A cells stably expressing p53 R273H untreated or treated with increasing concentrations of the indicated ROCK inhibitors for 24hrs. *n*=3 biologically independent replicates. **(c)** IC_{50} of the ROCK inhibitors for the indicated kinases [2-5]. *p* values were derived using two tailed *t*-tests from means± SD of *n*=3 independent experiments. $*p < 0.05$, $**p < 0.01$, $***p < 0.001$, $****p < 0.0001$. Source data with actual calculated *p* values are provided as Source Data file.

Supplementary Figure 6

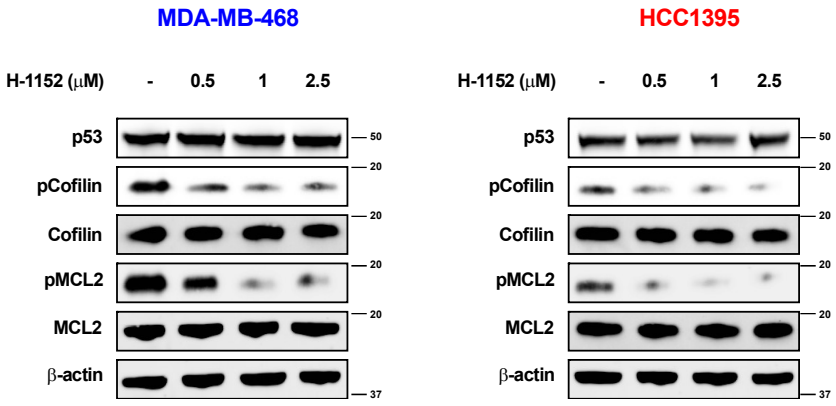

Supplementary Figure 6. H-1152 reduces phosphorylation levels of ROCK targets in tumor cells harboring p53 DNA contact or conformational mutations. Western blot analysis of whole cell lysates from MDA-MB-468 and HCC1395 cells either untreated or treated with increasing concentrations of H-1152 for 24hrs and probed with the indicated antibodies. β-actin was used as a loading control. Source data are provided as Source Data file.

Supplementary Figure 7

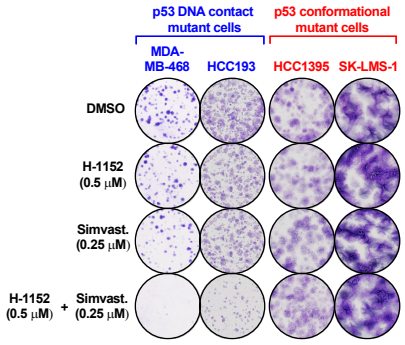

Supplementary Figure 7. H-1152 and Simvastatin cooperate to specifically inhibit cell growth of tumor lines harboring p53 DNA contact mutations. Representative plates from *n*=2 biologically independent replicates showing 2D colony formation by the indicated cell lines treated with DMSO or the indicated drugs every 2 days for 14 days.

Supplementary Figure 8

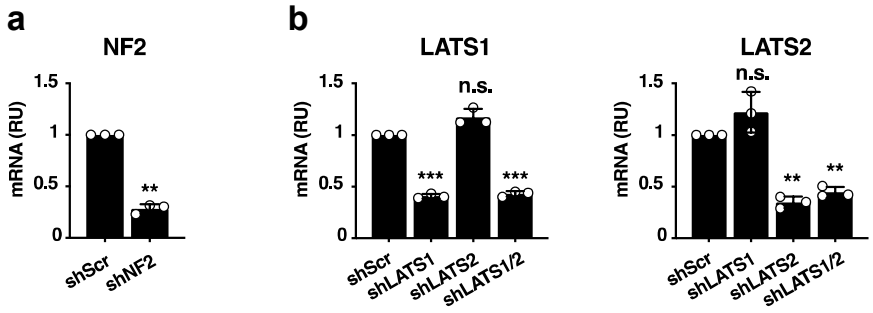

Supplementary Figure 8. NF2 and LATS1/2 knockdown in MCF10A cells. (a) mRNA expression levels of NF2 by real time PCR in MCF10A cells stably expressing shScr or shNF2. **(b)** mRNA expression levels of LATS1 or LATS2 by real time PCR in MCF10A cells stably expressing shScr, shLATS1, shLATS2 or shLATS1/2. *p* values were derived using two tailed *t*-tests from means± SD of *n*=3 independent experiments. $^{**}p < 0.01$, $^{***}p < 0.001$. Source data with actual calculated *p* values are provided as Source Data file.

Supplementary Figure 9

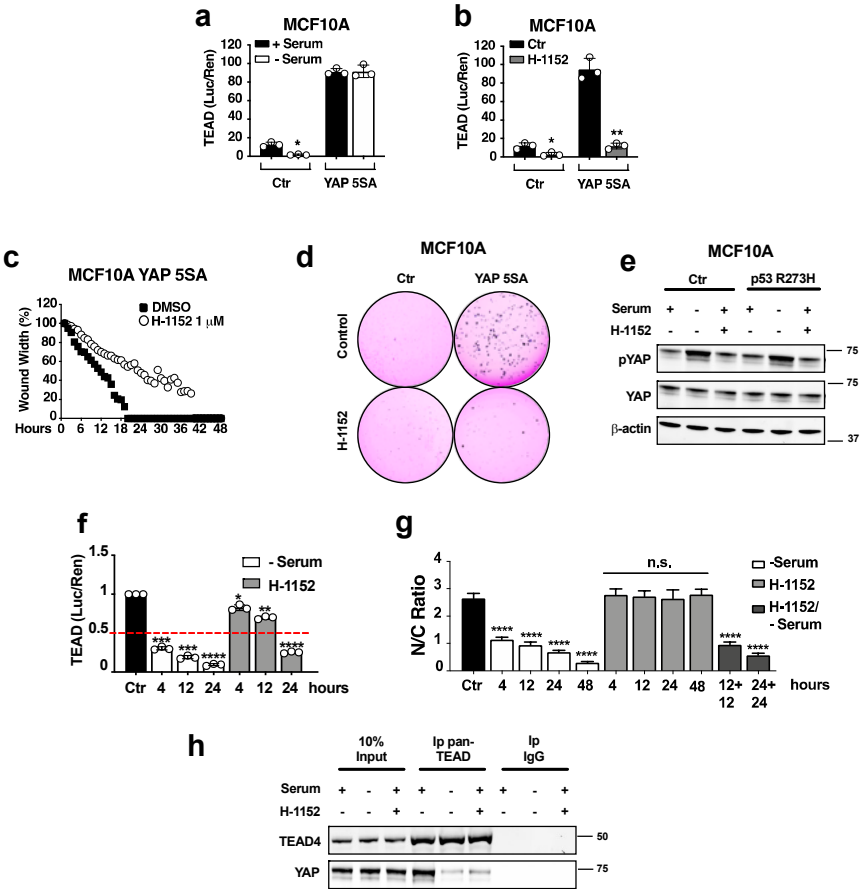

Supplementary Figure 9. ROCK inhibition antagonizes TEAD/YAP transcription and the transformed phenotype induced by YAP 5SA overexpression in MCF10A cells independently of YAP phosphorylation. (a and b) TEAD reporter activity of MCF10A cells expressing Empty Vector (Ctr) or YAP 5SA either in the presence or absence or serum for 24hrs **(a)** or untreated (Ctr) or treated with 1 μM H-1152 for 24hrs **(b)**. **(c)** *In vitro* migration measured by wound healing assay of MCF10A cells overexpressing YAP 5SA untreated or treated with 1 μM H-1152 for 48hrs. **(d)** Anchorage-independent growth in agar of the same cells as in **(c)** untreated or treated with 1 μM H-1152 every 4 days for 21 days. **(e)** Western blot analysis of whole cell lysates from MCF10A cells stably expressing EV control or p53 R273H untreated, treated with 1 μM H-1152 or serum starved for 24hrs and probed with the indicated antibodies. β-actin was used as a loading control. **(f)** TEAD reporter activity of MCF10A cells either untreated (Ctr), serum deprived or treated with 1 μM H-1152 in the presence of serum for the indicated time points. **(g)** Nucleo-cytoplasmic ratio (N/C ratio) of YAP in MCF10A cells either untreated (Ctr) or treated with 1 μM H-1152 in the presence or absence or serum for the indicated time points. Quantification of N/C ratio by confocal microscopy was determined as described in Methods. $n>100$ cells analyzed for each treatment condition **(h)** Co-immunoprecipitation of endogenous YAP and TEAD4 in MCF10A cells either untreated, treated with 1 μM H-1152 or serum starved for 24hrs. IgG antibodies were used as a negative control. 10% of total cell lysate was used as Input. *p* values were derived using two tailed *t*-tests from means ± SD of $n=3$ independent experiments. $^{*}p < 0.05$, $^{**}p < 0.01$, $^{***}p < 0.001$, $^{****}p < 0.0001$. Source data with actual calculated *p* values are provided as Source Data file.

Supplementary Figure 10

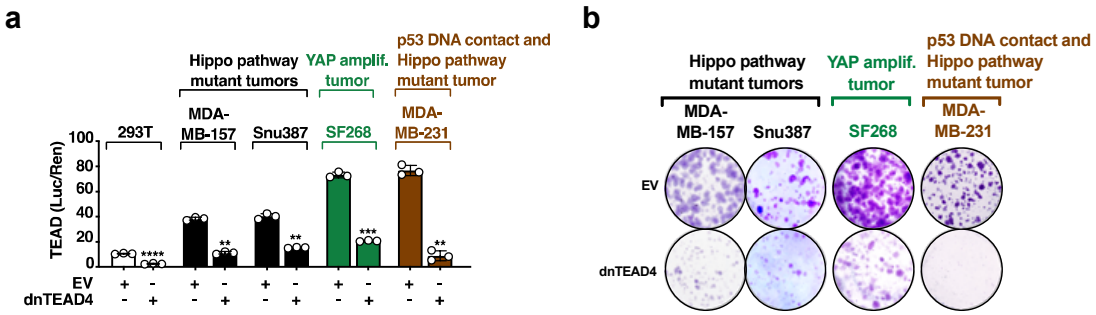

Supplementary Figure 10. Human tumor lines with Hippo pathway lesions and/or p53 DNA contact mutations exhibit high TEAD/YAP transcription and TEAD/YAP dependent 2D growth. (a) TEAD reporter activity of indicated tumor lines stably expressing empty vector control (EV) or dnTEAD4. **(b)** Representative plates showing 2D colony formation by indicated tumor lines stably expressing EV control or dnTEAD4 for 14 days. *p* values were derived using two tailed *t*-tests from means± SD of *n*=3 independent experiments. $^{**}p < 0.01$, $^{***}p < 0.001$, $^{****}p < 0.0001$. Source data with actual calculated *p* values are provided as Source Data file.

Supplementary Figure 11

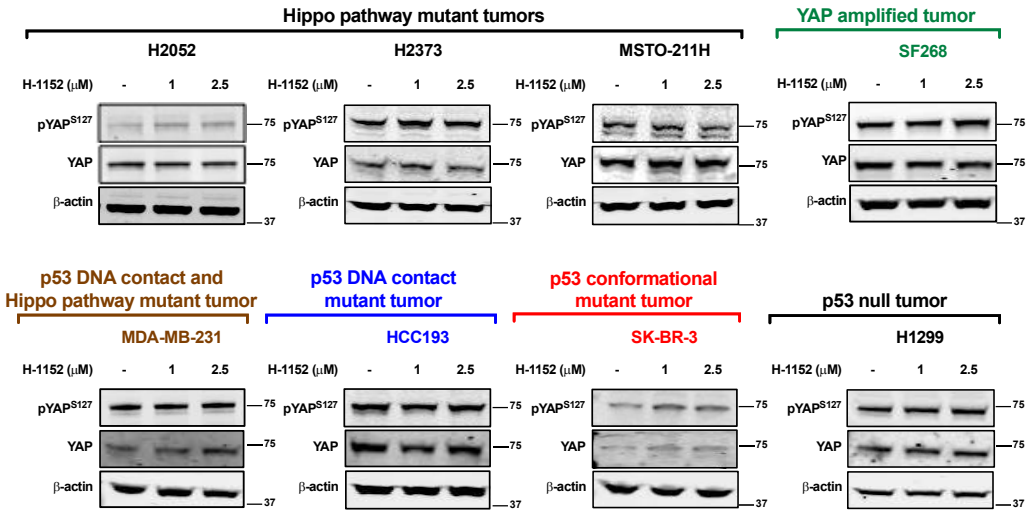

Supplementary Figure 11. ROCK inhibition does not affect pYAP^{S127} in human tumor cells. Western blot analysis of indicated tumor lines untreated or treated with 1 μM H-1152 for 24h and then probed with antibodies against YAP^{S127} and YAP. β-actin was used as a loading control. Results are representative of one of *n*=2 independent experiments**.** Source data are provided as Source Data file.

Supplementary Figure 12

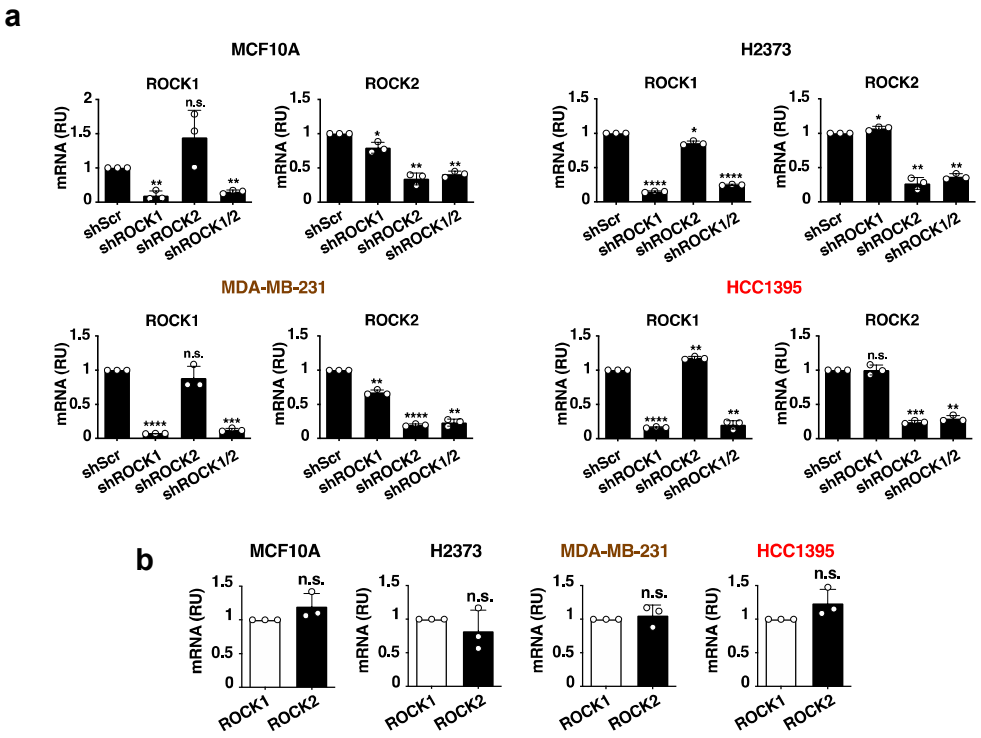

Supplementary Figure 12. ROCK1 and 2 knockdown in MCF10A cells and human tumor cells. (a) mRNA expression levels of ROCK1 or ROCK2 by real time PCR in the indicated cells stably expressing shScr, shROCK1, shROCK2 or shROCK1/2. **(b)** mRNA expression levels of ROCK1 and ROCK2 by real time PCR in the indicated cell lines. *p* values were derived using two tailed *t*-tests from means± SD of *n*=3 independent experiments. **p* < 0.05, ***p* < 0.01, ****p* < 0.001, *****p* < 0.0001. Source data with actual calculated p values are provided as Source Data file.

Supplementary Figure 13

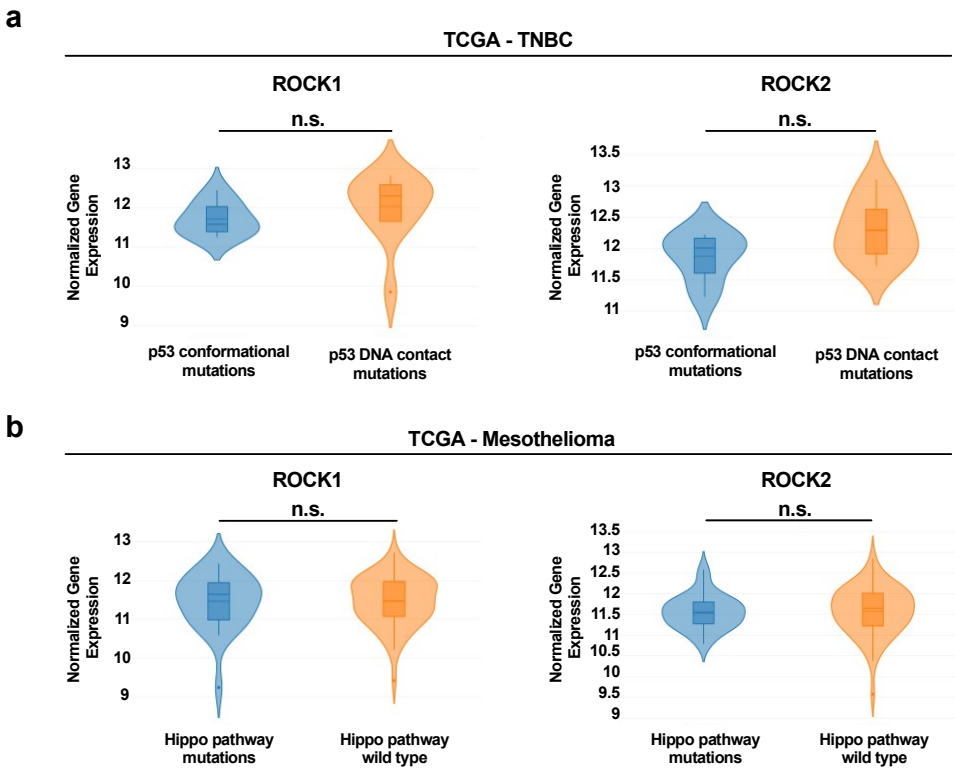

Supplementary Figure 13. ROCK1 and ROCK2 are equally expressed in patient samples exhibiting low and high TEAD/YAP transcriptional activity. ROCK1 and ROCK2 levels in patients samples from **(a)** TNBC and **(b)** mesothelioma TCGA databases. TNBC dataset was stratified based on *TP53* status according to DNA contact mutations or conformational mutations, while Mesothelioma dataset was stratified based on mutations in Hippo pathway core components, NF2 and LATS1/2. Boxplots show median and the inter quartile range (IQR) of the underlying data with whiskers extending to ± 1.5 IQR from boxes and dotted lines denote the mean. All outliers are shown as dots. *p*= *n.s* (not significant) calculated using two tailed *t*-test.

Supplementary Figure 14

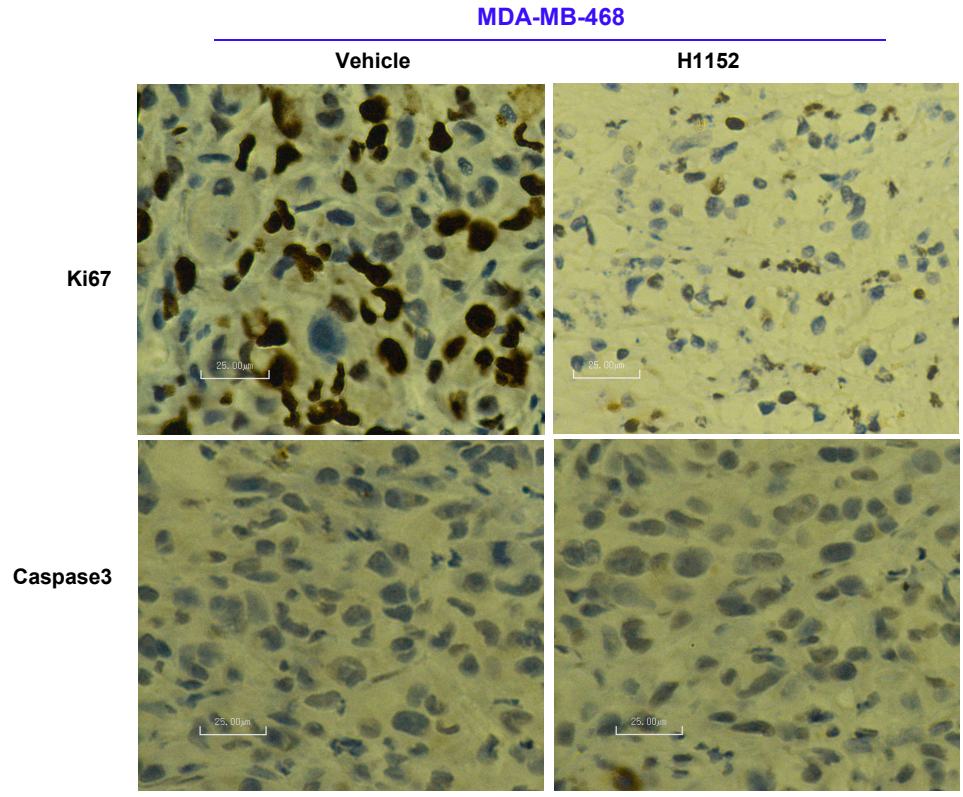

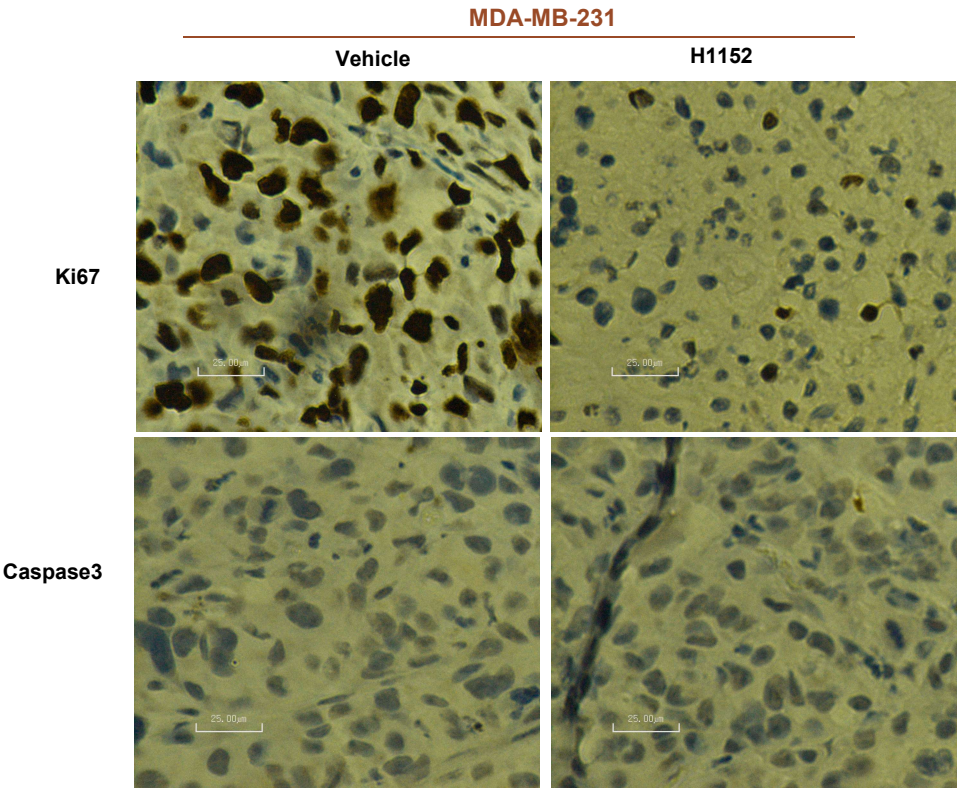

Supplementary Figure 14. ROCK inhibition antagonizes *in vivo* growth in the absence of apoptosis in human tumors with high TEAD/YAP transcription. Immunostaining of tumor sections from **(Fig. 5a and b)** with antibodies directed against Ki67 or caspase3 as described in the Methods. Scale bar: 25 μM, *n*=5 biologically independent mice per treatment group.

Supplementary Figure 15

a

p53 DNA contact vs. p53 conformational mutations in TNBC

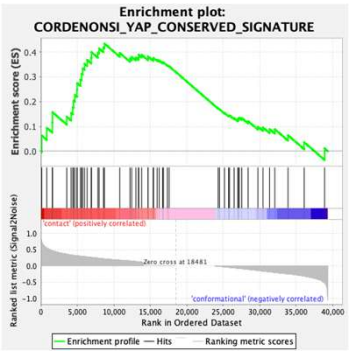

FDR q-value: 0.183

b

Hippo pathway mutations vs. Hippo pathway WT in Mesothelioma

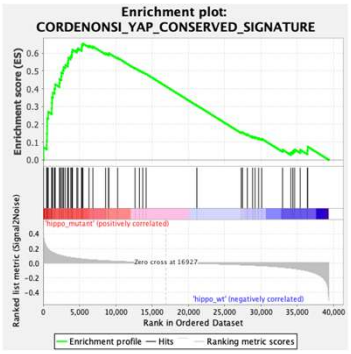

FDR q-value: 0.034

Supplementary Figure 15. Hippo pathway signature is enriched in patient samples with p53 DNA contact mutations or Hippo pathway mutations. Gene Set Enrichment Analysis (GSEA) for expression of TEAD/YAP gene signature in RNAseq data from **(a)** TNBC and **(b)** Mesothelioma patients. TNBC dataset was stratified based on *TP53* status according to DNA contact mutations or conformational mutations, while Mesothelioma dataset was stratified based on mutations in Hippo pathway core components, NF2 and LATS1/2 or not.

Supplementary Figure 16

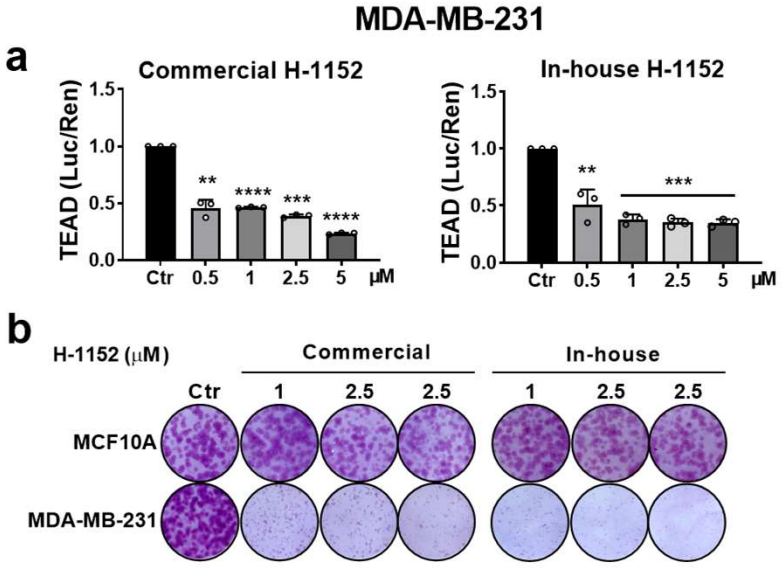

Supplementary Figure 16. In house synthesized H1152 and commercial H1152 show comparable potency in inhibiting TEAD/YAP activated cells. **(a)** TEAD reporter activity of MDA-MB-231 cells treated with increasing concentrations of In house synthesized or commercial H1152. **(b)** Representative plates showing 2D colony formation by MCF10A and MDA-MB-231 cells treated with 1μM and 2.5 μM of In house synthesized or commercial H1152. . *p* values were derived using two tailed *t*-tests from means± SD of *n*=3 independent experiments. $*p < 0.05$, $**p < 0.01$, $***p < 0.001$, $****p < 0.0001$. Source data with actual calculated *p* values are provided as Source Data file.

Supplementary References

1. Gao, J. *et al.* Integrative analysis of complex cancer genomics and clinical profiles using the cBioPortal. *Sci Signal* **6**, pl1, doi:10.1126/scisignal.2004088 (2013).
2. Tamura, M. *et al.* Development of specific Rho-kinase inhibitors and their clinical application. *Biochim Biophys Acta* **1754**, 245-252, doi:10.1016/j.bbapap.2005.06.015 (2005).
3. Goodman, K. B. *et al.* Development of dihydropyridone indazole amides as selective Rho-kinase inhibitors. *J Med Chem* **50**, 6-9, doi:10.1021/jm0609014 (2007).
4. Morwick, T. *et al.* Hit to lead account of the discovery of bisbenzamide and related ureidobenzamide inhibitors of Rho kinase. *J Med Chem* **53**, 759-777, doi:10.1021/jm9014263 (2010).
5. Uehata, M. *et al.* Calcium sensitization of smooth muscle mediated by a Rho-associated protein kinase in hypertension. *Nature* **389**, 990-994, doi:10.1038/40187 (1997).